Received: 29 September 2017 | Accepted: 30 April 2018

DOI: 10.1002/jcp.26816

ORIGINAL RESEARCH ARTICLE

WILEY Journal of Cellular Physiology

Effect of CCNB1 silencing on cell cycle, senescence, and apoptosis through the p53 signaling pathway in pancreatic cancer

Hui Zhang[1,2*] | Xuan Zhang[3*] | Xun Li[1,2] | Wen-Bo Meng[1,2] | Zhong-Tian Bai[1,2] | Shao-Zhen Rui[1,2] | Zheng-Feng Wang[1,2] | Wen-Ce Zhou[1,2] | Xiao-Da Jin[4]

[1]The Second Department of General Surgery, the First Hospital of Lanzhou University, Institute of Hepatopancreatobiliary Surgery of Gansu, Lanzhou, P. R. China

[2]Key Laboratory of Biotherapy and Regenerative Medicine of Gansu Province, Lanzhou, P. R. China

[3]Northwest Minzu University, Lanzhou, P. R. China

[4]University of South China, Hengyang, P. R. China

Correspondence
Wen-Ce Zhou and and Xun Li, The Second Department of General Surgery, the First Hospital of Lanzhou University, Institute of Hepatopancreatobiliary Surgery of Gansu, Key Laboratory of Biotherapy and Regenerative Medicine of Gansu Province, No. 1, Donggang West Road, Chengguan District, Lanzhou 730000, Gansu Province, P. R. China.
Email: zhouwc129@163.com (Wen-Ce Zhou); lxdr21@126.com (Xun Li)

Funding information
Gansu Provincial Natural Science Funds, Grant/Award Number: 1606RJZA139; Key Research and Development Program of Gansu, Grant/Award Number: 17YF1FA128; Gansu Province Science Foundation for Distinguished Young Scholars, Grant/Award Number: 1606RJDA317

Pancreatic cancer (PC) is a serious malignancy with high mortality and poor prognosis due to nonspecific incipient symptoms and early metastasis. Also, increasing evidence indicates that a panel of genes is newly identified in the pathogenesis of PC. As is a regulatory subunit, elevated cyclin B1 (CCNB1) expression has been detected in different cancers including PC. This study is designed to investigate the effects of CCNB1 silencing on cell cycle, senescence, and apoptosis through the p53 signaling pathway in PC. PC tissues and normal pancreatic tissues were collected. Cells were transfected and assigned into different groups. The expressions of CCNB1, p53, MDM2, Bax, caspase-9, caspase-3, and p21 in tissues and cells were detected by reverse transcription quantitative polymerase chain reaction and western blot analysis. β-Galactosidase staining, MTT assay, and flow cytometry were conducted to test cell senescence, proliferation, cell cycle, and apoptosis. PC tissues showed higher expressions of CCNB1 and MDM2 and lower expressions of Bax, caspase-9, caspase-3, and p21. Cells transfected with shCCNB1 had lower expressions of CCNB1 and MDM2, whereas higher expressions of Bax, caspase-9, caspase-3, p53, and p21. The shCCNB1 group had decreased proliferation and S-phase cell proportion and increased apoptosis, senescence, and G0/G1-phase cell proportion. The PFT-α group showed higher expressions of MDM2 and lower expressions of Bax, caspase-9, caspase-3, p53, and p21. The PFT-α group had increased proliferation and S-phase cell proportion and declined apoptosis, senescence, and G0/G1-phase cell proportion. CCNB1 silencing inhibits cell proliferation and promotes cell senescence via activation of the p53 signaling pathway in PC.

KEYWORDS
apoptosis, CCNB1, cell cycle, gene silencing, p53 signaling pathway, pancreatic cancer, senescence

1 | INTRODUCTION

Pancreatic cancer (PC) is one of the deadliest malignancies with poor prognosis as a result of nonspecific incipient symptoms and early metastasis (Y. Liu, Xia, & Zhong, 2014). PC is the fourth common cancerous cause of death, though its incidence is lower than that of many other types of cancers (Yadav & Lowenfels, 2013). Up to 2012, PC had registered an incidence rate of 7.28 per 100,000 in registration areas in China, and the age-specific incidence rate of PC drastically increased above the age of 40 years in China and peaked at the age of

*Hui Zhang and Xuan Zhang are regarded as co-first authors.

around 80 years (Lin, Yang, Jin, & Fu, 2015). Although the pathogenesis and etiology of PC remain to be fully elucidated, some common risk factors for PC have been reported, including smoking, obesity, genetics, diabetes, diet, inactivity, body mass index, and even pancreatitis and alcohol consumption (Ilic & Ilic, 2016; Wolfgang et al., 2013; H. Zhang et al., 2018). Treatments for PC include surgery, radiation therapy, chemotherapy, and palliative care, which are optioned depending on the PC stage in a multidisciplinary approach (Kamisawa, Wood, Itoi, & Takaori, 2016). However, outcomes of sophisticated PC surgeries or combination of therapies have improved modestly for patients and more efficient treatments are desperately demanded (Rossi, Rehman, & Gondi, 2014). Moreover, PC patients eligible for surgery constitute less than 15% of the total, making gene therapy a new widely investigated therapeutic approach (Y. Liu et al., 2014).

Cyclins refer to proteins that differ in their levels to activate specific cyclin-dependent kinases (CDKs) required for progression in the cell cycle (Shin et al., 2012). Cyclin B1 (CCNB1) has a pivotal role in regulating and forming a complex with CDK1 to promote the transition from the G2 phase of cell cycle to mitosis (Fang, Yu, Liang, Xu, & Cai, 2014). Increasing evidence demonstrates that the overexpression of CCNB1 is observed in certain number of human cancers including colorectal cancer, breast cancer, and PC (Fang et al., 2014; Nimeus-Malmstrom et al., 2010; Zhou et al., 2014). Located on chromosome 17p, p53 regulates DNA repair, cell cycle, apoptosis, and senescence and therefore plays an important role in genomic stability maintenance and tumor prevention (J. Liu, Zhang, Hu, & Feng, 2015; Zhao et al., 2016). The p53 tumor suppressor gene mutates in more than 50% of human malignancies (Zhao et al., 2016) and is mutated in 50–75% of PC cells (Morton et al., 2010). Moreover, the p53 tumor suppressor pathway is also pivotal in mediating the response of commonly used cancer therapies (Grochola, Zeron-Medina, Meriaux, & Bond, 2010). A previous study shows that PC patients compounded with p53 deletion in peritoneal drainage need a more adjuvant treatment (Kang et al., 2013). Despite significant research on the cellular and molecular signaling pathways in PC cells, few efficient therapies have been developed and utilized to target these pathways (Rossi et al., 2014). Moreover, the association between CCNB1 and the p53 signaling pathway has not been investigated in PC. In this study, we explore the effect of CCNB1 silencing on cell cycle, senescence, and apoptosis through the p53 signaling pathway in PC.

2 | MATERIALS AND METHODS

2.1 | Ethical statement

This study was approved by the ethics committee of the First Hospital of Lanzhou University. Patients and their families signed the informed consent.

2.2 | Study subjects

The PC tissues (PC group) were consisted of 40 resected specimens (16 from female patients and 24 from male patients; aged 35–73 years) and pathologically confirmed as PC by the Second Department of General Surgery of the First Hospital of Lanzhou University from November 1, 2011 to November 30, 2016. In accordance with the International Union Against Cancer (IUCC) staging system in 2002 (Sandvik, Soreide, Gudlaugsson, Kvaloy, & Soreide, 2016), the PC tissues were classified as follows: 6 in stage I, 10 in stage II, 12 in stage II, and 12 in stage IV; 17 of low differentiation, 11 of moderate differentiation, and 12 of high differentiation. Normal pancreas tissues (normal pancreas group) were collected from 14 volunteers (8 males and 6 females, aged 34–67 years) from October 1, 2011 to November 30, 2016. Of the 14 normal specimens, 5 were preserved in a liver transplantation procedure and 9 were obtained in other upper abdominal surgeries (trauma laparotomy and cholecystectomy). The age and sex ratios of each group are well-matched. All resected specimens were timely preserved in liquid nitrogen.

2.3 | Hematoxylin–eosin (H&E) staining

Part of the PC and normal pancreas tissues was fixed with 4% paraformaldehyde for 24 hr and dehydrated by 80%, 90%, and 100% ethanol and butanol successively. Tissues were further embedded with paraffin at 60°C and cut into 5-μm-serial sections. After being spread out and collected at 45°C, the sections were baked for 1 hr at 60°C and dewaxed with xylene. Tissues were stained with H&E after hydration. The prepared sections were dewaxed and dehydrated with gradient ethanol and stained by hematoxylin (Beijing Solarbio Science & Technology Co. Ltd., Beijing, China) for 2 min. After being washed by running water for 10 s, the sections were differentiated with 1% hydrochloric acid–ethanol mixture for 10 s. The sections were subsequently washed with distilled water for 1 min and dehydrated with eosin for 1 min. The sections were rewashed with distilled water for 10 s, dehydrated with gradient ethanol, cleaned with xylene and then mounted with neutral gum. Finally, the morphological changes of tissues were observed with optical microscopy (XP-330; Shanghai Bingyu Optical Instrument Co. Ltd., Shanghai, China).

2.4 | Immunohistochemistry for CCNB1-positive expression rate

The PC and normal pancreas tissues were fixed with formaldehyde, embedded in paraffin, and cut into 4-μm serial sections. The sections were baked in a 60°C incubator for 1 hr, conventionally dewaxed with xylene, dehydrated with gradient ethanol and then immersed in 3% H_2O_2 for 10 min. The sections were subsequently washed with distilled water, placed at a high pressure for 90 s for antigen retrieval, cooled at room temperature and washed with phosphate-buffered saline (PBS). After that, the sections were further blocked with 5% bovine serum albumin and incubated at 37°C for 30 min. The sections were added with diluted primary antibody rabbit anti-human CCNB1 (1:500, EPR17060; Abcam Inc., Cambridge, MA) for incubation at 4°C overnight, followed by PBS washing. Then, the sections were added with the diluted biotin-labeled immunoglobulin G (IgG) secondary antibody (1:100; HY90046; Shanghai HengYuan Biological Technology

Co. Ltd., Shanghai, China) for incubation at 37°C for 30 min, followed by PBS washing. The sections were added with streptomycin avidin–peroxidase solution (Zhongshan Biotechnology Co. Ltd., Beijing, China) for incubating for 30 min at 37°C. After PBS washing, the sections were visualized with chromogen 3,3-diaminobenzidine (DAB; Beijing Bioss Biotech, Beijing, China), immersed in hematoxylin for 5 min and rewashed with running water. Subsequently, the sections were washed with 1% hydrochloric acid-ethanol and turned blue with running water for 20 min. Five high-magnification fields of view (×400) on each section were randomly selected, and the positive expression rate of the CCNB1 protein was measured by the proportion of positive cells to a total of 100 cells on each view: PC positive cell number/total PC cell number >10% was marked as positive (+); PC positive cell number <10% was marked as negative (−). The experiment was repeated three times.

2.5 | Cell culture

Primary cells in normal pancreatic tissues and PC tissues were isolated and extracted to conduct the in vitro cell experiment with the purchased Capan-2 PC cell line. Part of the samples was treated with 0.25% trypsin for 30 min. After the trypsin was discarded, tissues were treated with 0.1% type I collagenase until they turned into suspensions. The cells were sieved through a 100-mesh metallic screen, washed with cold Hanks' solution one time, and cultured in Roswell Park Memorial Institute (RPMI) 1640 medium (Gibco, Gaitherburg, MD) with 10% fetal bovine serum (FBS) in a 5% CO_2 incubator at 37°C. The suspensions were further treated with 0.25% trypsin (Gibco), dissociated into single cell suspensions using RPMI 1640 medium supplemented with 10% FBS, and cultured regularly for passage. Cells in the logarithmic growth phase were chosen for subsequent experiment.

2.6 | CCNB1 shRNA vector construction

According to the CCNB1 complementary DNA (cDNA) sequence reported by GenBank, the forward and reverse primers were designed and synthesized. The CCNB1 target gene fragment was obtained through PCR amplification with cDNA as template. Three groups of shCCNB1 (shCCNB1-1, shCCNB1-2, and shCCNB1-3) were designed according to the obtained gene fragment. After electrophoresis with agarose gel, the purified shCCNB1 (pshCCNB1) PCR product and gene-marked pTrack-CMV plasmid were digested by *Bgl*II and *Sal*I, respectively. Then, the target fragments were recovered by the gel extraction kit and then ligated with T4 DNA ligase overnight. The *Escherichia coli* competent cells were transformed using calcium chloride, and the monoclonal cells were selected afterward. PCR, dual-enzyme digestion, and gene sequencing were performed to identify the target fragment. The empty vectors and pshCCNB1-1, pshCCNB1-2, and pshCCNB1-3 obtained through gene sequencing (Table 1) were linearized with *Pme*I. Recombinant adenovirus vectors of CCNB1 shRNA were acquired through identification of positive clones using enzyme digestion and were subsequently transformed into *E. coli* competent cells, and the positive clones were amplified.

TABLE 1 Target gene sequences for interference

ShRNA	Target sequence
CCNB1-1	CCATTATTGATCGGTTCAT
CCNB1-2	GCAGCACCTGGCTAAGAAT
CCNB1-3	CCACATCGAAGCATGCTAA
NC	TCGTTATGCCCAAATACCCA

Note. NC, negative control.

2.7 | CCNB1 shRNA transfection

The PC cells were divided into negative control (NC; transfected with NC vector), pshCCNB1-1 (transfected with pshCCNB1-1 vector), pshCCNB1-2 (transfected with pshCCNB1-2 vector), and pshCCNB1-3 (transfected with pshCCNB1-3 vector) groups. Before transfection, the cell passage was conducted and cells were inoculated in a six-well plate with 2×10^6 cells in each well. The next day after transfection, cells were cultured in 250 μl of serum-free Opti-MEM (51985042; Gibco) as they reached 70–80% confluence. The plasmid was prepared according to the instructions of the manufacturer of the Lipofectamine® 2000 transfection reagent (11668-019; Invitrogen, New York, CA), and 4 μg of plasmid was diluted with 250 μl of Opti-MEM. The Lipofectamine® 2000 and plasmid complex were added into the plate ready for transfection. The medium was refreshed 6 hr after transfection. Forty-eight hours after transfection, the transfection rate was detected under a fluorescence microscope, and the messenger RNA (mRNA) and protein expressions of CCNB1 were evaluated by reverse transcription quantitative polymerase chain reaction (RT-qPCR) and western blot analysis, respectively. The CCNB1 shRNA vector with the strongest interference was then selected for subsequent study.

2.8 | Cell grouping

The above PC and normal pancreas primary cells and the Capan-2 PC cell line after passage were divided into normal (normal primary cells, without any treatment), blank (PC primary cells or Capan-2 PC cells, without any treatment), NC (PC primary cells or Capan-2 PC cells transfected with the NC vector), shCCNB1 (PC primary cells or Capan-2 PC cells transfected with pshCCNB1-1), PFT-α (during PC primary cells or Capan-2 PC cell culturing, 10 μM PFT-α was added, which was a p53 inhibitor), and PFT-α + shCCNB1 (PC primary cells or Capan-2 PC cells, transfected with PFT-α + pshCCNB1-1) groups. Before transfection, cell passage was conducted and the cells were inoculated in a six-well plate with 1×10^5 cells in each well. The cells reached 70–80% confluency at the day of transfection, and the cell transfection was conducted in accordance with the instructions of the manufacturer of the Lipofectamine® 2000 transfection reagent (11668-019; Invitrogen). The serum-free Opti-MEM (250 μl, 51985042; Gibco) was used to dilute solutions (100 ng each) with

empty plasmid, NC-small interfering (siRNA)-CCNB1, and siRNA-CCNB1 (50 nM final concentration) and thoroughly mixed, and the medium complex was then incubated at room temperature for 5 min. Another 250 μl of serum-free Opti-MEM was used to dilute 5 μl of Lipofectamine® 2000. The above two diluted medium complexes were then mixed together, incubated for 5 min at room temperature, and then added into the plate. After transfection, cells were further cultured in a 5% CO_2 incubator at 37℃. Six to eight hours later, the medium was refreshed. After 24–28 hr incubation, the subsequent experiment was conducted.

2.9 | RT-qPCR

Part of the PC and normal pancreas tissues was added into liquid nitrogen and ground into fine powder (or collecting cells). Total RNA was extracted through Trizol methods (15596-018; Invitrogen), and its concentration and purity were evaluated. The sample RNA was reversely transcripted into cDNA according to the instructions of the manufacturer of the Primescript™ RT reagent kit (RRO37A; Takara, Dalian, Liaoning, China) in a reaction system of 25 μl. Conditions for reaction were as follows: reverse transcription at 37℃ for 15 min and inactivation of reverse transcriptase at 85℃ for 5 s. The acquired cDNA was diluted and mixed thoroughly with 65 μl of diethyl pyrocarbonate–treated water and subsequently amplified by RT-qPCR in accordance with the instructions of the manufacturer of the SYBR® Premix Ex Taq™ II reagent kit (Takara). The reaction system was 50 μl containing 25 μl of SYBR® Premix Ex Taq™ II (2×), 2 μl of PCR reverse and forward primers (10 μM) each, l μl of ROX Reference Dye (50×), 4 μl of DNA template, and 16 μl of dH_2O. RT-qPCR was performed in an ABI PRISM® 7300 system (Applied Biosystems, Foster City, CA), and conditions for RT-qPCR were as follows: predenaturation at 95℃ for 4 min, denaturation at 94℃ for 30 s, annealing at 58℃ for 30 s, and extension at 72℃ for 1 min with a total of 40 cycles. β-Actin was taken as the internal reference, and all primers (Table 2) were designed and synthesized by Bio Just (Wuhan, China). $2^{-\Delta\Delta C_t}$ referred to the expression ratio of the target genes between the experiment and control group, and following was the formula: $\Delta\Delta C_t = \Delta C_{t\ (\text{experiment group})} - \Delta C_{t\ (\text{control group})}$, and $\Delta C_t = C_{t\ (\text{target gene})} - C_{t\ (\beta\text{-actin})}$ (Pagani et al., 2014). The cycle threshold (C_t) referred to the cycle number logarithmically amplified when the real-time fluorescence intensity reached the threshold value. The experiment was repeated three times.

2.10 | Western blot analysis

Part of the PC and normal pancreas tissues was frozen with liquid nitrogen and ground into fine powder (or collecting cells) and was further added with 1 ml of lysis buffer (composed of 50 mmol/L Tris, 150 mmol/L NaCl, 5 mmol/L ethylenediamine tetraacetic acid [EDTA], 0.1% sodium dodecyl sulfate [SDS], 1% NP-40, 5 μg/ml Aprotinin, and 2 mmol/L phenylmethylsulfonyl fluoride [PMSF]). After that, the tissues underwent ice bath and made into a homogenate, which was then lysed with the protein lysis buffer at 4℃ for 30 min (shaken every 10 min). The homogenate was further centrifuged at 12,000 r/min for 20 min at 4℃ with lipid layer discarded and supernatant collected. The concentration of protein of each sample was measured by the bicinchoninic acid (BCA) protein assay reagent kit (20201ES76; Yeasen, Shanghai, China). Deionized water was used to adjust the loading buffer with 30 μg for each protein lane. An SDS separation gel (10%) and a concentrated gel (4%) were prepared. The samples were blended with the sample loading buffer. The mixtures were successively boiled at 100℃ for 5 min, ice-bathed, centrifuged, and added equally into each lane by a micropipette for electrophoretic separation. Subsequently, the extracted protein was transferred onto the nitrocellulose membranes, which were fixed with 5% skim milk powder at 4℃ overnight. The membranes were incubated overnight with the following diluted rabbit polyclonal antibodies as primary antibodies: CCNB1 (ab32053; Abcam; 1:3,000–1:20,000), p53 (ab32049; Abcam; 1:1,000–1:5,000), phosphorylated (p)-p53 (ab183547; Abcam; 1:1,000), mouse double minute 2 (MDM2; ab38618; Abcam; 1:1,000), Bax (ab32503; Abcam; 1:1,000–1:1,000), caspase-9 (ab32539; Abcam; 1:1,000–1:1,000), caspase-3 (ab13847; Abcam; 1:500), or p21 (ab109520; Abcam; 1:1,000–1:10,000). After one-night incubation, the membranes were washed with PBS three times (5 min each), added with horseradish peroxidase-labeled goat antirabbit IgG (1:1,000; Boster, Wuhan, China) as the secondary antibody, and incubated for 1 hr at 37℃. The membranes were subsequently rewashed with PBS three times (5 min each) and immersed in chemiluminescence (ECL; Pierce, Waltham, MA) for 1 min at room temperature. With the liquid being discarded, the membranes were covered by a preservative film. Then, the results were observed after X-ray exposure, development, and

TABLE 2 Primer sequence of CCNB1, p53, 21 MDM2, Bax, caspase-3, and caspase-9

Gene	Primer sequence (5′-3′)
CCNB1	Forward: GCACTTTCCTCCTTCTCA
	Reverse: CGATGTGGCATACTTGTT
p53	Forward: AGAGCTGAATGAGGCCTTGGAA
	Reverse: GAGTCAGGCCCTTCTGTCTTGAAC
p21	Forward: AAACGGGAACCAGGACAC
	Reverse: AGCAGCGGAACAAGGAGT
MDM2	Forward: TGGGCAGCTTGAAGCAGTTG
	Reverse: CAGGCTGCCATGTGACCTAAGA
Bax	Forward: TTTCTGACGGCAACTTCAACTG
	Reverse: CAACCACCCTGGTCTTGGAT
caspase-3	Forward: CATGGCCTGTCAGAAAATAC
	Reverse: TAACCCGAGTAAGAATGTGC
caspase-9	Forward: TTCCCAGGTTTTGTTTCCTG
	Reverse: CCTTTCACCGAAACAGCATT
β-actin	Forward: AGCGAGCATCCCCCAAAGTT
	Reverse: GGGCACGAAGGCTCATCATT

Note. CCNB1, Cyclin B1; MDM2, murine double minute 2.

fixation of membranes in a dark environment. β-Actin was taken as the internal reference, and the ratio of the gray-scale values of the target band to the internal reference band was taken as the relative expression of protein.

2.11 | β-Galactosidase staining

The PC cells in the logarithmic growth phase (1×10^5) were taken and seeded in a 12-well plate. The cell senescence of each group was detected using β-galactosidase staining after 48-hr culturing. With the medium being discarded, the cells were washed with PBS and fixed with a β-galactosidase staining fixative for 15 min at room temperature. Afterward, the fixative was removed and the plate was rewashed with PBS before being added with 500 μl of working solution for staining. The plate was sealed with a preservative film and incubated overnight at 37°C. The working solution was then removed, and the plate was observed and pictured under optical microscopy. Consequently, cell senescence was marked by the senescence index (SI) of the cells in each group: SI = number of cells with positively expressed β-galactosidase/number of total cells ×100%.

2.12 | MTT assay

The transfected cells of each group were cultured in RPMI 1640 medium supplemented with 10% FBS with a concentration of 5×10^3 cells/μl for incubation in a 5% CO_2 incubator at 37°C for 48 hr. The cells in the logarithmic growth phase were selected for digestion at room temperature, and the cell suspension was transferred into a centrifuge tube and dissociated into single cells with a sterile pipette for counting the cell number. The cells were transferred into a 96-well plate with 5,000 cells in each well (in strict accordance with the counted number) and incubated in a 5% CO_2 incubator at 37°C. After the medium was refreshed, peripheral wells were supplemented with PBS in case of evaporation. The plate was then incubated for 0, 24, 48, or 72 hr in a 5% CO_2 incubator at 37°C. After incubation, the plate was added with 20 μl of MTT in each well in a dark environment. After thorough mixing, the plate was again incubated in a 5% CO_2 incubator at 37°C for 4 hr and centrifuged at 1500 rpm for 5 min afterward. With the removal of the supernatant, 150 μl of dimethylsulfoxide solution was added into the plate, which was shaken on an orbital platform for 30 min at 37°C in a dark environment. Subsequently, the optical density (OD) value at 490 nm was evaluated by a microplate reader (Multiskan GO, Thermo Fisher Scientific Inc., Waltham, MA). The cell growth curve was graphed with the MTT processing time as the horizontal axis and OD value as the vertical axis.

2.13 | Flow cytometry

Forty-eight hours after transfection, the cells were washed with cold PBS three times. Then, with the supernatant being discarded through centrifugation, the cells were resuspended at 1×10^5 cells/ml in PBS. Precooled (at −20°C) 75% ethanol was dripped into the cell suspension for fixation. After 1 hr fixation at 4°C, cold ethanol was discarded by centrifugation and the cells were washed with PBS twice. With the removal of the supernatant, the cells were then added with 100 μl RNase A in the dark, underwent water bath at 37°C for 30 min, and stained with 400 μl of propidium iodide (PI; Sigma, St. Louis, MO) for 30 min at 4°C in a dark environment. CytoFLEX flow cytometry (CA 92821; Beckman Coulter, Fullerton, CA) was applied to record the red fluorescence at an excitation wavelength of 488 nm to analyze the cell cycle.

Forty-eight hours after transfection, the cells were digested with trypsin containing no EDTA, collected in a flow tube, and centrifuged to remove the supernatant. The cells were washed three times with cold PBS, and the supernatant was again removed through centrifugation. In accordance with the instructions of the manufacturer of the annexin-V-FITC apoptosis detection reagent kit (Sigma), annexin-V–FITC–PI was prepared with annexin-V–FITC, PI, and (4-(2-hydroxyethyl)-1-piperazineethanesulfonic acid) HEPES buffers at 1:2:50. Then, every 100 μl of dye liquor was used to resuspend 1×10^5 cells. After thorough mixing, the cells were incubated at room temperature for 15 min and added with 1 ml of HEPES buffer. A wavelength of 488 nm was applied to excite a 525 and a 620 nm bandpass filter to detect the FITC and PI fluorescence, respectively, and subsequently to measure cell apoptosis.

2.14 | Statistical analysis

The collected data were processed by SPSS 21.0 (SPSS, Chicago, IL). The measurement data was expressed as mean ± standard deviation (*SD*). The χ^2 test was conducted to observe the correlation between the expression of CCNB1 and the clinicopathological features of PC. The *t* test was applied for comparison between two groups and analysis of variance (ANOVA) for comparison among groups. Statistical significance was represented by $p < 0.05$.

3 | RESULTS

3.1 | Pathological characteristics of PC and normal pancreas tissues

The result of pathological examination (Figure 1) showed that normal pancreas tissues were clear in structure and nonmalignant in morphology with no obvious inflammatory cell infiltration or interstitial connective tissue hyperplasia. PC tissues displayed clear fibroplasia, atrophy, and disappearance of acinar, obvious inflammatory cell infiltration and

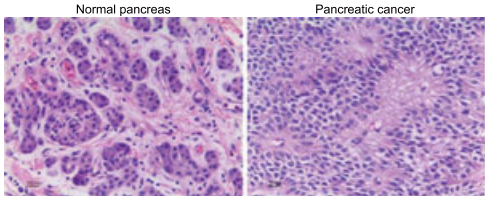

FIGURE 1 H&E staining results of PC and normal pancreas tissues. H&E, hematoxylin–eosin; PC, pancreatic cancer [Color figure can be viewed at wileyonlinelibrary.com]

interstitial connective tissue hyperplasia. The ductal epithelial cell of PC tissue penetrated the basement membrane, thus causing tumorigenesis.

3.2 | CCNB1 protein expression was higher in PC tissues

The positive expression rate of the CCNB1 protein was (12.00 ± 1.89%) in normal pancreas tissues, whereas (68.00 ± 14.43%) in PC tissues (Figure 2). Therefore, the positive expression rate of CCNB1 was significantly higher in PC tissues than in normal pancreas tissues ($p < 0.05$).

3.3 | Protein expression of CCNB1 showed significant difference in differentiation of PC tissues with different degrees

The expression of CCNB1 was significantly increased in 40 cases of PC tissues, and the expression level was obviously different. The number of positive cells in 40% cases was less than 10% with low expression, and the number of positive cells in 60% cases varied from 10% to 80% with high expression. No difference was found among the protein expressions of CCNB1 with age, gender, tumor site, and TNM staging in different groups, but the protein expression of CCNB1 indicated significant difference in differentiation of PC tissues with different degrees (Table 3).

High expression of CCNB1 was mainly found in well-differentiated adenocarcinoma, which accounted for 59.25% of PC patients with high expression (16/27), whereas moderately differentiated adenocarcinoma and poorly differentiated adenocarcinoma accounted for 18.52% (5/27) and 22.22% (6/27), respectively. Among the patients with low expression of CCNB1, well-, moderately, and poorly differentiated adenocarcinomas accounted for 7.69% (1/13), 46.15% (6/13), and 46.15% (6/13), respectively. In moderately and poorly differentiated adenocarcinomas, low expression of CCNB1 was found in 50% (6/12) and 50% (6/12), respectively, whereas well-differentiated adenocarcinomas only accounted for 5.88% (1/17), which is lower than that for moderately differentiated adenocarcinoma ($\chi^2 = 8.435$; $p < 0.01$) and poorly differentiated adenocarcinoma ($\chi^2 = 7.477$; $p < 0.01$).

TABLE 3 Correlation between the expression of CCNB1 and the clinicopathological features of PC

Parameters	*n*	CCNB1 expression (%) + (≥10%)	CCNB1 expression (%) −(<10%)	χ^2	*P*
Overall	40	67.5 (27/40)	32.5 (13/40)		
Age (years)				0.311	0.557
<65	21	71.43 (15/21)	28.57 (6/21)		
≥65	19	63.16(12/19)	36.84(7/19)		
Gender				3.723	0.053
Male	24	79.17 (19/24)	20.83 (5/24)		
Female	16	50 (8/16)	50 (8/16)		
Site				1.161	0.281
Head	29	72.41 (21/29)	27.59 (8/29)		
Body and/or tail	11	54.55 (6/11)	45.55 (5/11)		
TNM stage				0.019	0.888
I	6	50 (3/6)	50 (3/6)		
II	10	80 (8/10)	20 (2/10)		
III	13	69.23 (9/13)	30.77 (4/13)		
IV	11	63.64 (7/11)	36.36 (4/11)		
Grade				9.603	0.008
Well differentiated[1]	17	94.12 (16/17)	5.88 (1/17)		
Moderately differentiated[2]	11	45.45 (5/11)	54.55 (6/11)		
Poorly differentiated[3]	12	50 (6/12)	50 (6/12)		

Note. CCNB1, cyclin B1; PC, pancreatic cancer; 1 and 2, $\chi^2 = 7.234$; $p = 0.007$; 1 and 3, $\chi^2 = 8.435$; $p = 0.004$; 2 and 3, $\chi^2 = 0.111$; $p = 0.739$

3.4 | mRNA and protein expressions of CCNB1, MDM2, p53 mRNA, Bax, caspase-9, caspase-3, and p21 in normal pancreas and PC tissues

mRNA expressions of tissues from 14 normal patients and 40 PC patients were examined, and western blot analysis maps of protein expression were randomly selected from three normal pancreas and PC patients. Compared with normal pancreas tissues, PC tissues

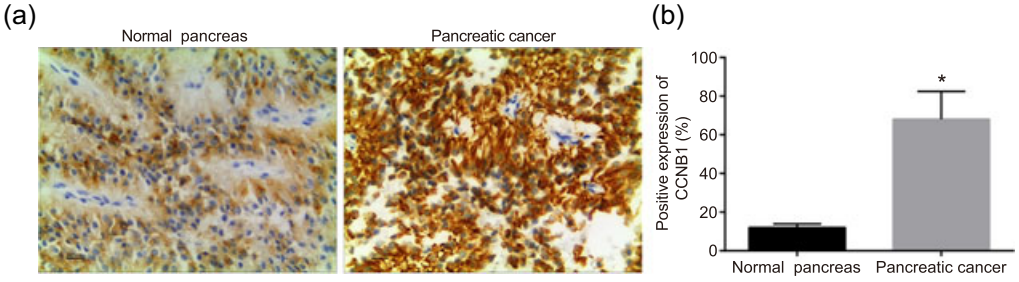

FIGURE 2 Immunohistochemistry reveals the positive expression of the CCNB1 protein in PC and normal pancreas tissues, and a higher positive expression of the CCNB1 protein is found in PC tissues. (a) Immunohistochemistry of normal pancreas tissues and PC tissues. (b) Comparison between the positive expressions of the CCNB1 protein in the PC tissues and in the normal pancreas tissues. *$p < 0.05$ compared with the normal pancreas tissues. PC, pancreatic cancer [Color figure can be viewed at wileyonlinelibrary.com]

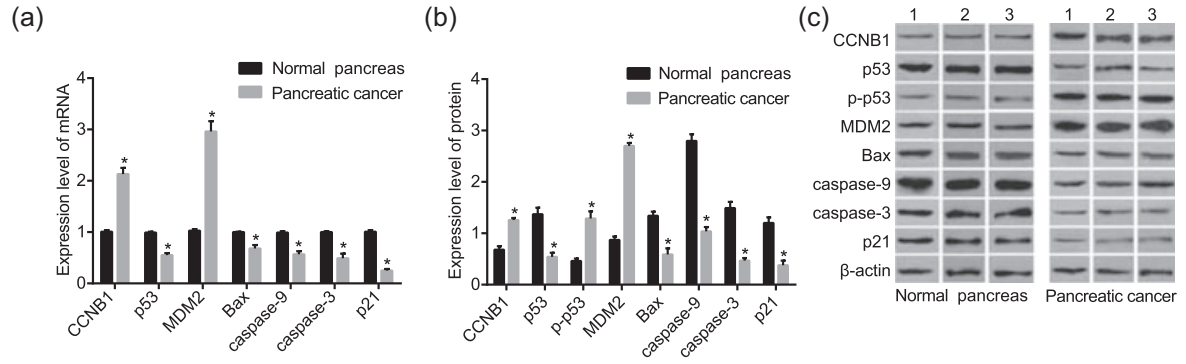

FIGURE 3 Messenger RNA (mRNA) and protein expressions of CCNB1, p53, MDM2, Bax, caspase-9, caspase-3, and p21 in PC and normal pancreas tissues. (a) mRNA expressions in PC and normal pancreas tissues. (b) Protein expressions in PC and normal pancreas tissues. (c) Western blot analysis map of protein expressions in 6 patients. *$p < 0.05$ compared with the normal pancreas tissues. PC, pancreatic cancer

showed significantly higher mRNA and protein expressions of CCNB1 and MDM2; significantly lower mRNA and protein expressions of Bax, caspase-9, caspase-3, p21, and p53; and a significantly lower protein expression of p-p53 ($p < 0.05$; Figure 3).

3.5 | pshCCNB1-1 vector had the strongest interference efficiency

The transfection efficiency of all vectors reached over 80%. Compared with that in the NC group, CCNB1 protein expression was significantly lower in the pshCCNB1-1, pshCCNB1-2, and pshCCNB1-3 groups ($p < 0.05$), with the pshCCNB1-1 group having the lowest CCNB1 protein expression (Figure 4). Consequently, pshCCNB1-1 was proved to have the strongest interference efficiency and was selected for subsequent experiment.

3.6 | mRNA and protein expressions of CCNB1, MDM2, p53, Bax, caspase-9, caspase-3, and p21 in normal and PC cells after transfection

RT-qPCR and western blot analysis were conducted to investigate the different mRNA and protein expressions of CCNB1, MDM2, p53, and other cells in normal and PC cells after transfection. Compared with those of the normal group, the mRNA and protein expressions of CCNB1 and MDM2 were significantly higher, the mRNA and protein expressions of Bax, caspase-9, caspase-3, p21, and p53 were significantly lower, and the protein expression of p-p53 was significantly lower in other five groups ($p < 0.05$). Compared with the blank group, the NC group showed no significantly different expressions of mRNA and protein; the shCCNB1 group exhibited significantly lower mRNA and protein expressions of CCNB1 and MDM2; significantly higher mRNA and protein expressions of Bax, caspase-9, caspase-3, p21, and p53; and a significantly higher protein expression of p-p53 ($p < 0.05$); the PFT-α group showed significantly higher mRNA and protein expressions of MDM2, significantly lower mRNA and protein expressions of Bax, caspase-9, caspase-3, p21, and p53, a significantly lower protein expression of p-p53, and no significantly different expression of CCNB1 ($p < 0.05$); and the PFT-α + shCCNB1 group exhibited a significantly lower expression of CCNB1 but no significantly different expression of other genes ($p > 0.05$; Figure 5).

3.7 | CCNB1 silencing promoted cell senescence

To study the relationship between CCNB1 silencing and cell senescence, the cell senescence in each group was observed after

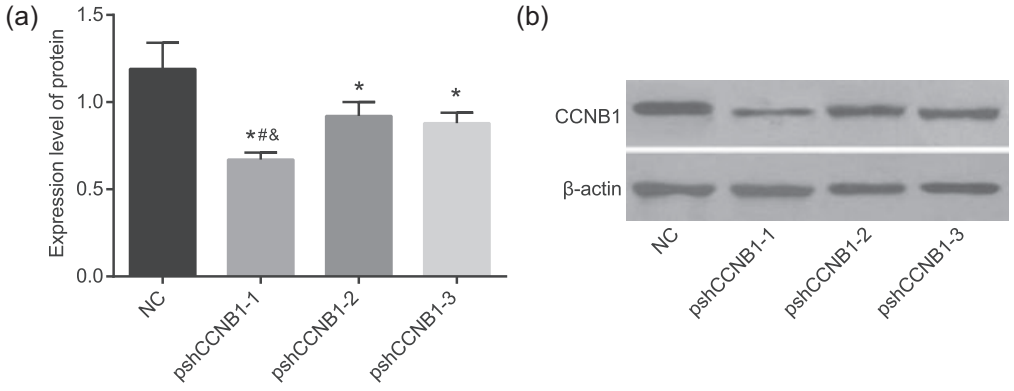

FIGURE 4 Expression of the CCNB1 protein in the NC, pshCCNB1-1, pshCCNB1-2, and pshCCNB1-3 groups, and pshCCNB1-1 was selected for the follow-up cell experiment. (a) Expression of the CCNB1 protein in each group. (b) Protein bands. *$p < 0.05$ compared with the blank group; $^{\#}p < 0.05$ compared with the pshCCNB1-2 group; $^{\&}p < 0.05$ compared with the pshCCNB1-3 group. NC, negative control

β-galactosidase staining. The staining results showed that cells in the blank, NC, and PFT-α + shCCNB1 groups grew at a high density and were in a diamond shape with observable nuclear division. Cells in the normal and shCCNB1 groups grew at a low density, and part of the cells was in a triangle and enlarged shape with observable vacuolar degeneration, indicating cell senescence. Cells in the PFT-α group grew at a high density with observable nuclear division. The result of β-galactosidase staining showed that compared to that in the normal group, SI was significantly lower in other groups. Compared to that in the blank and NC groups, SI increased significantly in the shCCNB1 group and decreased significantly in the PFT-α group ($p < 0.05$). No much significant difference was found between the blank group and the PFT-α + shCCNB1 group ($p > 0.05$; Figure 6). The results verified that CCNB1 silencing could promote cell senescence.

3.8 | CCNB1 silencing inhibited cell proliferation

Next, the cell proliferation in each group was studied in PC primary cells and Capan-2 PC cells. The MTT assay revealed that other groups had significantly increased cell proliferation when compared with that in the normal group ($p < 0.05$). In comparison with the blank group, the shCCNB1 group had significantly decreased cell proliferation, whereas the PFT-α group had significantly increased cell proliferation ($p < 0.05$) and the NC and PFT-α + shCCNB1 groups exhibited no significant difference in cell proliferation ($p > 0.05$; Figure 7). The results demonstrated that CCNB1 silencing could suppress cell proliferation.

3.9 | CCNB1 silencing arrested cells in the G0/G1 phase

In the following experiments, we mainly investigated the changes of cell cycle in each group. According to the results of flow cytometry, in comparison with the normal group, other groups displayed enhanced cell proportion in the S phase, declined cell proportion in the G0/G1 phase, and slowed cell cycle ($p < 0.05$). The NC and PFT-α + shCCNB1 groups showed no significant difference from the blank group ($p > 0.05$). In comparison with the blank group, the shCCNB1 group had increased cell proportion in the G0/G1 phase and decreased cell proportion in the S phase ($p < 0.05$), whereas the PFT-α group had increased cell proportion in the S phase and decreased cell proportion in the G0/G1 phase ($p < 0.05$; Figure 8). The results suggested that CCNB1 silencing arrested cells in the G0/G1 phase.

3.10 | CCNB1 silencing promoted cell apoptosis

Finally, flow cytometry was conducted to detect the effects of CCNB1 silencing on cell apoptosis. Compared with the normal group, other groups had a decreased cell apoptosis rate ($p < 0.05$). The NC and PFT-α + shCCNB1 groups displayed no significant difference in the cell apoptosis rate when compared with that in the blank group ($p > 0.05$). The shCCNB1 groups had a significantly increased cell apoptosis rate, whereas the PFT-α group had a significantly declined cell apoptosis rate when compared with that in the blank group

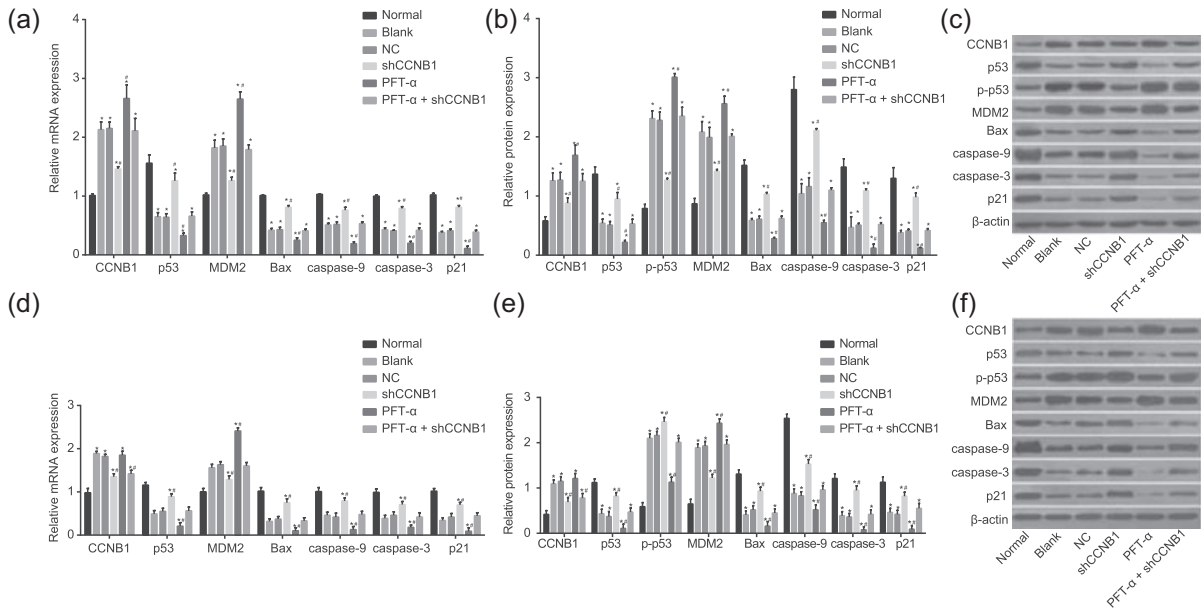

FIGURE 5 Comparisons of messenger RNA (mRNA) and protein expressions of CCNB1, p53, MDM2, Bax, caspase-9, caspase-3, and p21 among the normal, blank, NC, shCCNB1, PFT-α, and PFT-α + shCCNB1 groups. (a) mRNA expressions of CCNB1, p53, MDM2, Bax, caspase-9, caspase-3, and p21 of PC primary cells in each group. (b) Protein expressions of CCNB1, p53, MDM2, Bax, caspase-9, caspase-3, and p21 of PC primary cells in each group. (c) Protein bands of CCNB1, p53, MDM2, Bax, caspase-9, caspase-3, and p21 of PC primary cells. (d) mRNA expressions of CCNB1, p53, MDM2, Bax, caspase-9, caspase-3, and p21 of Capan-2 PC cells in each group. (e) Protein expressions of Capan-2 PC cells in each group. (f) Protein bands of CCNB1, p53, MDM2, Bax, caspase-9, caspase-3, and p21 of Capan-2 PC cells. $^{*}p < 0.05$ compared with the normal group; $^{\#}p < 0.05$ compared with the blank group. NC, negative control; PC, pancreatic cancer

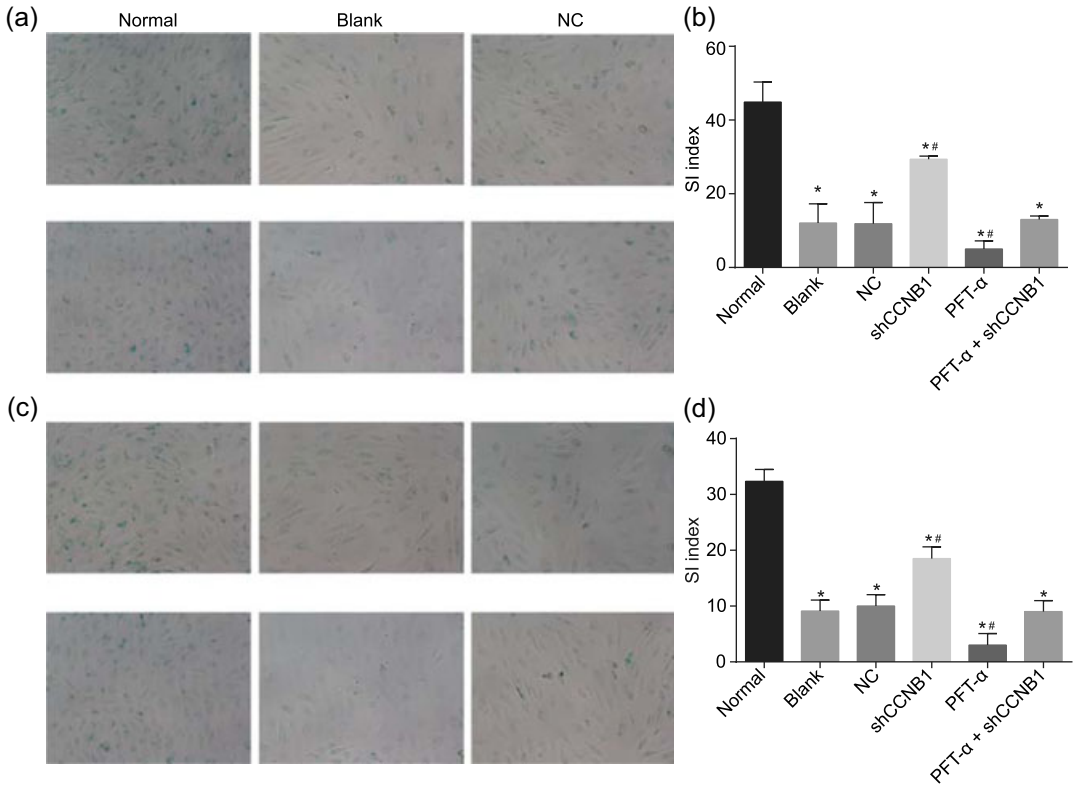

FIGURE 6 β-Galactosidase staining shows that CCNB1 silencing promotes cell senescence. (a) Staining of PC primary cells in each group. (b) Senescence index of PC primary cells in each group. (c) Staining of Capan-2 PC cells in each group. (d) Ssenescence index of Capan-2 PC cells in each group. $^{*}p < 0.05$ compared with the normal group; $^{\#}p < 0.05$ compared with the blank group. NC, negative control; PC, pancreatic cancer [Color figure can be viewed at wileyonlinelibrary.com]

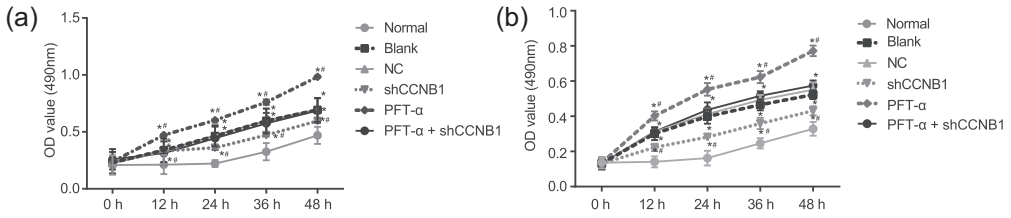

FIGURE 7 MTT assay indicates that CCNB1 silencing inhibits cell proliferation. (a) Cell proliferation of PC primary cells in each group. (b) Cell proliferation of Capan-2 PC cells in each group. $^{*}p < 0.05$ compared with the normal group; $^{\#}p < 0.05$ compared with the blank group. NC, negative control; PC, pancreatic cancer

($p < 0.05$; Figure 9). The results revealed that CCNB1 silencing promoted cell apoptosis.

4 | DISCUSSION

Currently, there are a number of promising therapies for PC treatment, whereas the promise for the development of safer and more therapeutic targets depends rather on a thorough understanding of the molecular aberrations (Chiorean & Coveler, 2015; Mohammed, Van Buren, & Fisher, 2014). Among them, CCNB1 expression is identified to be a useful marker of poor prognosis of PC patients (Shin et al., 2012), whereas the potential of the interaction between CCNB1 and p53 expression in PC has not been discussed. Our current study demonstrates that CCNB1 silencing activates the p53 signaling pathway and consequently inhibits cell proliferation and promotes cell senescence in PC.

The result of our experiment showed that expressions of CCNB1 and MDM2 elevated, whereas expressions of Bax, caspase-9, caspase-3, and p21 reduced in PC tissues compared with those in normal pancreas tissues. CCNB1 is known to have a key role in Cdk1 regulation and initiates G2 to mitosis progression (Khan et al., 2013). The overexpression of CCNB1 is involved in several cancers such as renal, breast, and PCs (Ding, Li, Zou, Zou, & Wang, 2014; Ikuerowo et al., 2006; Zhou et al., 2014). MDM2 is an oncoprotein, which blocks p53-mediated transactivation (Mendoza, Mandani, & Momand, 2014) and has been revealed to be amplified in PC (Dong et al., 2005). Bax is known as a

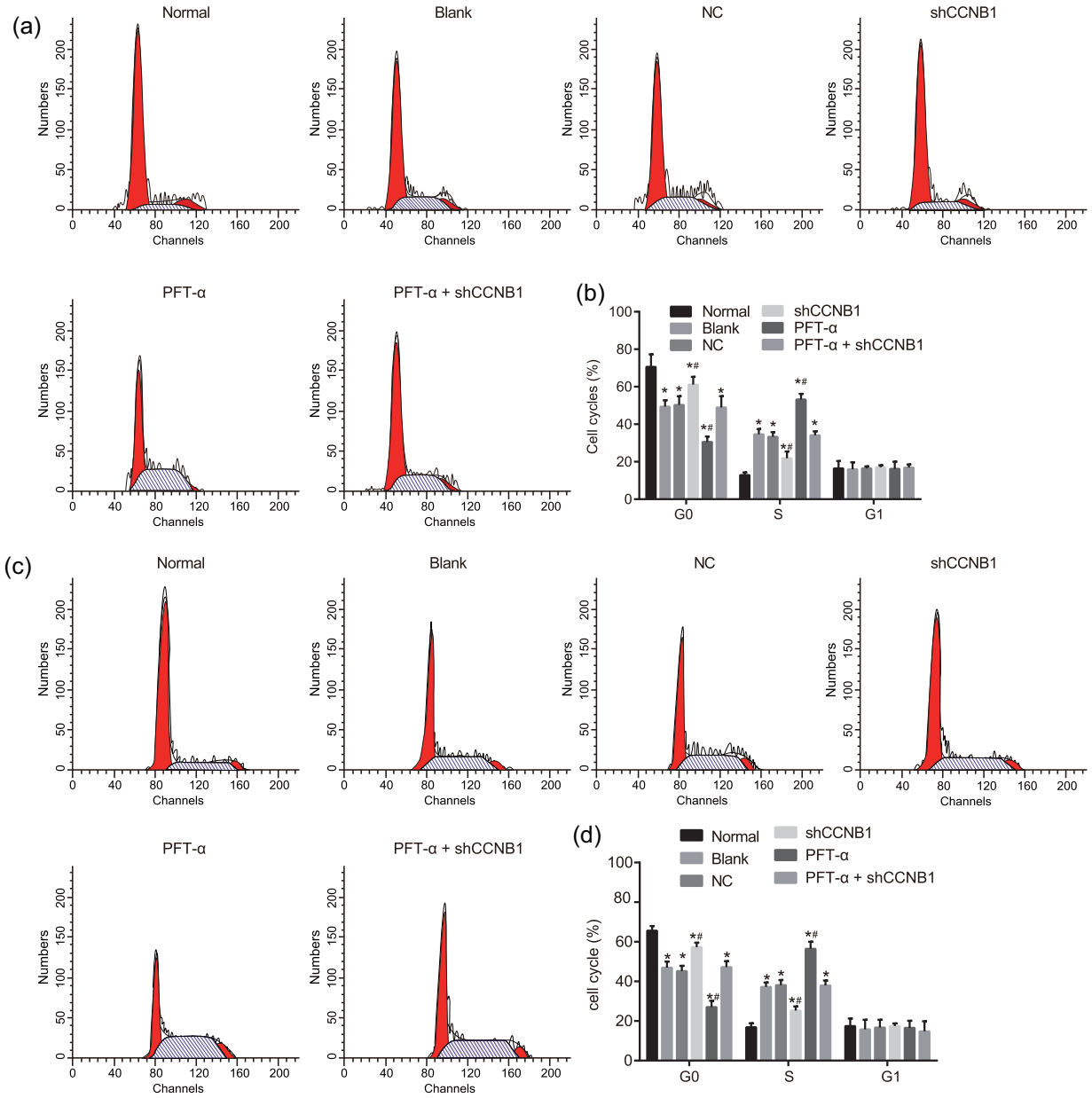

FIGURE 8 Flow cytometry reveals that CCNB1 silencing arrests cells in the G0/G1 phase. (a) Cell cycle flow chart of PC primary cells in each group. (b) Cell cycle histogram of PC primary cells in each group. (c) Cell cycle flow chart of Capan-2 PC cells in each group. (d) Cell cycle histogram of Capan-2 PC cells in each group. $^{*}p < 0.05$ compared with the normal group; $^{\#}p < 0.05$ compared with the blank group. NC, negative control; PC, pancreatic cancer [Color figure can be viewed at wileyonlinelibrary.com]

multidomain proapoptotic protein, and its higher expression signifies better outcomes for PC patients (Haneef, Parvathy, Thankayyan, Sithul, & Sreeharshan, 2012; J. J. Zhang et al., 2016). p21 is a crucial target gene of p53 in executing cell cycle arrest (Y. Zhang et al., 2014). Previous evidence shows that low expression of p21 corresponds to poor prognosis in PC patients (Sun, Yang, Sun, & Chen, 2014). Caspases is a class of proteases that play a significant role in cell apoptosis (Ding & Nguyen, 2013). To be specific, caspase-9 is the initiator, whereas caspase-3 is the executioner of apoptosis (Frejlich et al., 2013). A previous study demonstrates that the activation of caspase-3 is associated with the reduced progression of PC cells (Srivastava et al., 2015). Also, the activation of caspase-9 is associated with the apoptotic mechanism of PC cells (Singh, Nawale, Sarkar, & Suresh, 2016).

In addition, our study reported that CCNB1 silencing in PC cells suppressed the expressions of CCNB1 and MDM2, whereas increased the expressions of Bax, capspase-3 and capspase-9, p53, and p21. On the contrary, p53 inhibition in PC enhanced the expression of MDM2, whereas decreased the expressions of Bax, capspase-3, capspase-9, p53, and p21. Likewise, studies have shown that inhibiting CCNB1 reactivates and increases p53 expression in cervical cancer (Kreis et al., 2010), and reactivation of the p53 pathway in PC has been confirmed to be accompanied with MDM2 repression (Azmi et al., 2010). Bax has been reported to be directly

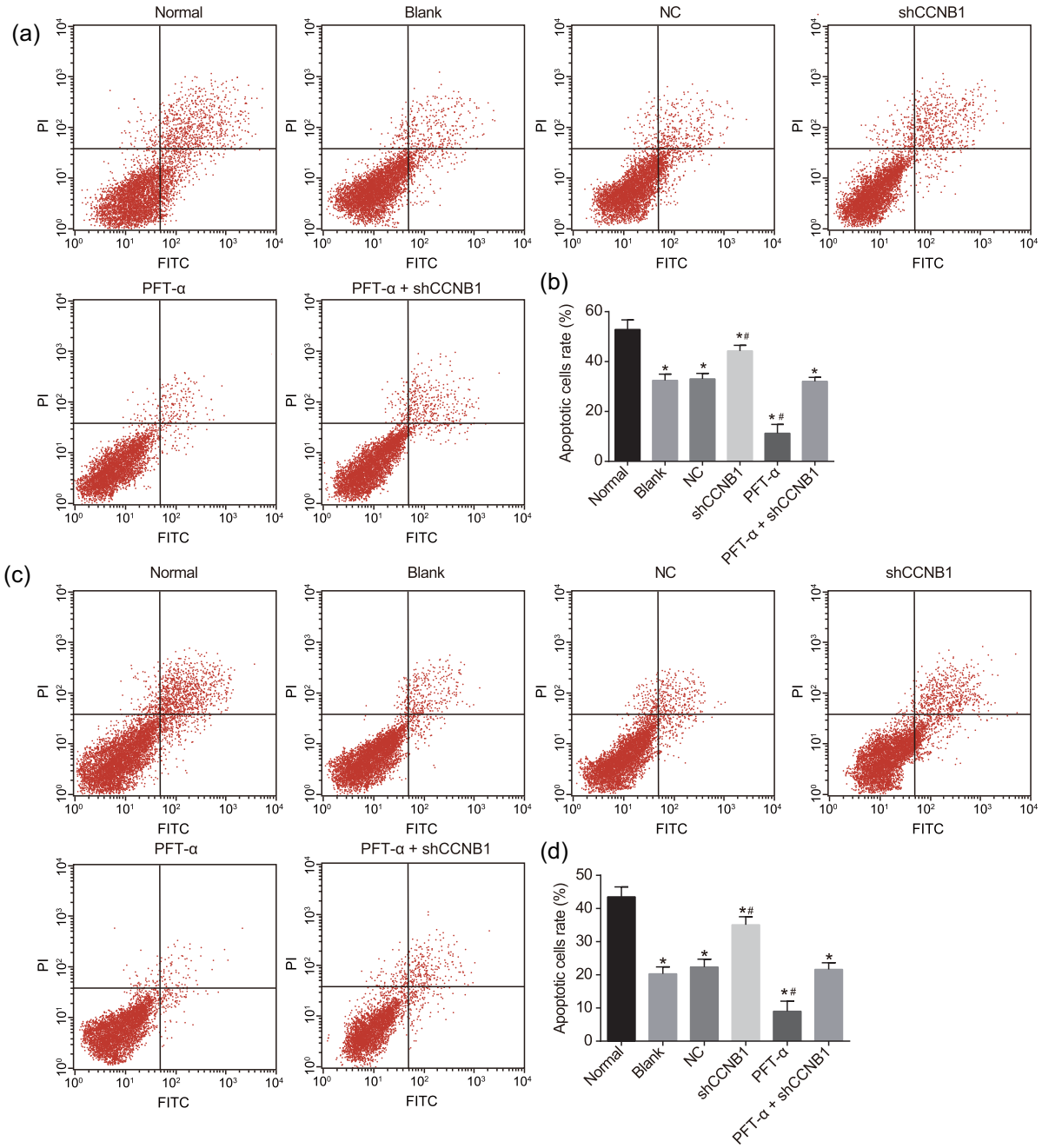

FIGURE 9 Flow cytometry suggests that CCNB1 silencing promotes cell apoptosis. (a) Cell apoptosis flow chart of PC primary cells in each group. (b) Cell apoptosis histogram of PC primary cells in each group. (c) Cell apoptosis flow chart of Capan-2 PC cells in each group. (d) Cell apoptosis histogram of Capan-2 PC cells in each group. $^{*}p < 0.05$ compared with the normal group; $^{\#}p < 0.05$ compared with the blank group. NC, negative control; PC, pancreatic cancer [Color figure can be viewed at wileyonlinelibrary.com]

activated by p53 without the presence of other proteins to permeablize mitochondria and engage the apoptotic program (Chipuk et al., 2004). Moreover, p53-induced apoptosis involves triggering the caspase-9 initiator and its downstream caspase-3 executioner (Wong, Morse, & Zhitkovich, 2013). The increased p53 expression has been shown to be accompanied with a marked increase of caspase-3 and caspase-9 expressions in breast cancer treatment (Alhazmi et al., 2014). p53 induces p21 through direct binding to its promoter (Suzuki, Ito, Ikeda, & Tamura, 2012). The induction of p21 arrests the cell cycle in the G1 phase and, in this way, mediates the function of p53 (Sivonova et al., 2015). Overall, it shows that reactivation of p53 and regulation of apoptosis-related proteins are inducible via CCNB1 silencing.

Consequently, we found that cells transfected with shCCNB1 had elevated G0/G1 cell proportion, cell senescence, and cell apoptosis, whereas cells transfected with PFT-α presented the opposite case. The observed results are consistent with previous studies, which have shown that downregulation of CCNB1 expression induces cell

cycle blockage and impaired proliferation of B16-F10 cells (Kedinger et al., 2013) and inhibition of CCNB1 and Cdk1 expressions contributes to G2/M phase cell cycle arrest and growth inhibition in gastric cancer SGC-7901 cells (Gao, Li, Qu, Zhu, & Ji, 2014). According to Wang et al. (2014), phosphorylation of mitochondrial substrates mediated by CCNB1/Cdk1 allows cells to react to an increased energy requirement for G2 to mitosis transition and to upregulate mitochondrial respiration for a successful progression of cell cycle. A study reports that p53 can inhibit malignant transformation by triggering the cell-autonomous program of apoptosis or cell-cycle arrest and noncell autonomous program of cellular senescence through secreted factors that regulate the macrophage function (Lujambio et al., 2013). Moreover, the activation of p53 has been confirmed to be associated with inhibition of PC cell proliferation (Hu et al., 2016). Therefore, the possibility that CCNB1 silencing prevents PC cell progression via p53 signaling pathway activation follows strictly the previous finding.

In conclusion, our current study identifies the important role of CCNB1 silencing in inhibiting cell proliferation and inducing cell senescence and apoptosis via the p53 signaling pathway. Although our findings have significant implication for therapeutic development in PC treatment, the mechanism mediating the interaction between CCNB1 and p53 in PC still demands further elucidation.

ACKNOWLEDGEMENTS

The work was supported by the Gansu Provincial Natural Science Funds (Grant No. 1606RJZA139), Key Research and Development Program of Gansu (Grant No. 17YF1FA128), and the Gansu Province Science Foundation for Distinguished Young Scholars (Grant No. 1606RJDA317). We would also like to thank all participants enrolled in the current study. We would like to express our gratitude to those who provided technical assistance and valuable advice.

CONFLICTS OF INTEREST

The authors declare that there are no conflicts of interest.

ORCID

Wen-Ce Zhou http://orcid.org/0000-0003-2573-9170

REFERENCES

Alhazmi, M. I., Hasan, T. N., Shafi, G., Al-Assaf, A. H., Alfawaz, M. A., & Alshatwi, A. A. (2014). Roles of p53 and caspases in induction of apoptosis in MCF-7 breast cancer cells treated with a methanolic extract of *Nigella sativa* seeds. *Asian Pacific Journal of Cancer Prevention*, *15*(22), 9655–9660.

Azmi, A. S., Philip, P. A., Aboukameel, A., Wang, Z., Banerjee, S., Zafar, S. F., … Mohammad, R. M. (2010). Reactivation of p53 by novel MDM2 inhibitors: Implications for pancreatic cancer therapy. *Current Cancer Drug Targets*, *10*(3), 319–331.

Chiorean, E. G., & Coveler, A. L. (2015). Pancreatic cancer: Optimizing treatment options, new, and emerging targeted therapies. *Drug Design, Development and Therapy*, *9*, 3529–3545.

Chipuk, J. E., Kuwana, T., Bouchier-Hayes, L., Droin, N. M., Newmeyer, D. D., Schuler, M., & Green, D. R. (2004). Direct activation of Bax by p53 mediates mitochondrial membrane permeabilization and apoptosis. *Science*, *303*(5660), 1010–1014.

Ding, K., Li, W., Zou, Z., Zou, X., & Wang, C. (2014). CCNB1 is a prognostic biomarker for ER+ breast cancer. *Medical Hypotheses*, *83*(3), 359–364.

Ding, Y., & Nguyen, T. A. (2013). PQ1, a quinoline derivative, induces apoptosis in T47D breast cancer cells through activation of caspase-8 and caspase-9. *Apoptosis*, *18*(9), 1071–1082.

Dong, M., Ma, G., Tu, W., Guo, K. J., Tian, Y. L., & Dong, Y. T. (2005). Clinicopathological significance of p53 and mdm2 protein expression in human pancreatic cancer. *World Journal of Gastroenterology*, *11*(14), 2162–2165.

Fang, Y., Yu, H., Liang, X., Xu, J., & Cai, X. (2014). Chk1-induced CCNB1 overexpression promotes cell proliferation and tumor growth in human colorectal cancer. *Cancer Biology & Therapy*, *15*(9), 1268–1279.

Frejlich, E., Rudno-Rudzinska, J., Janiszewski, K., Salomon, L., Kotulski, K., Pelzer, O., … Kielan, W. (2013). Caspases and their role in gastric cancer. *Advances in Clinical and Experimental Medicine*, *22*(4), 593–602.

Gao, S. Y., Li, J., Qu, X. Y., Zhu, N., & Ji, Y. B. (2014). Downregulation of Cdk1 and cyclinB1 expression contributes to oridonin-induced cell cycle arrest at G2/M phase and growth inhibition in SGC-7901 gastric cancer cells. *Asian Pacific Journal of Cancer Prevention*, *15*(15), 6437–6441.

Grochola, L. F., Zeron-Medina, J., Meriaux, S., & Bond, G. L. (2010). Single-nucleotide polymorphisms in the p53 signaling pathway. *Cold Spring Harbor Perspectives in Biology*, *2*(5), a001032–a001032.

Haneef, J., Parvathy, M., Thankayyan, R. S., Sithul, H., & Sreeharshan, S. (2012). Bax translocation mediated mitochondrial apoptosis and caspase dependent photosensitizing effect of Ficus religiosa on cancer cells. *PLoS One*, *7*(7), e40055.

Hu, D., Su, C., Jiang, M., Shen, Y., Shi, A., Zhao, F., … Tang, W. (2016). Fenofibrate inhibited pancreatic cancer cells proliferation via activation of p53 mediated by upregulation of LncRNA MEG3. *Biochemical and Biophysical Research Communications*, *471*(2), 290–295.

Ikuerowo, S. O., Kuczyk, M. A., Mengel, M., van der Heyde, E., Shittu, O. B., Vaske, B., … Serth, J. (2006). Alteration of subcellular and cellular expression patterns of cyclin B1 in renal cell carcinoma is significantly related to clinical progression and survival of patients. *International Journal of Cancer*, *119*(4), 867–874.

Ilic, M., & Ilic, I. (2016). Epidemiology of pancreatic cancer. *World Journal of Gastroenterology*, *22*(44), 9694–9705.

Kamisawa, T., Wood, L. D., Itoi, T., & Takaori, K. (2016). Pancreatic cancer. *Lancet*, *388*(10039), 73–85.

Kang, M. J., Han, S. S., Jang, J. Y., Park, J. W., Kwon, W., Chang, Y. R., & Kim, S. W. (2013). Cancer cells with p53 deletion detected by fluorescent in situ hybridization in peritoneal drainage fluid is correlated with early peritoneal seeding in resectable pancreatic cancer. *Journal of the Korean Surgical Society*, *84*(4), 209–215.

Kedinger, V., Meulle, A., Zounib, O., Bonnet, M. E., Gossart, J. B., Benoit, E., … Bolcato-Bellemin, A. L. (2013). Sticky siRNAs targeting survivin and cyclin B1 exert an antitumoral effect on melanoma subcutaneous xenografts and lung metastases. *BMC Cancer*, *13*, 338.

Khan, S., Brougham, C. L., Ryan, J., Sahrudin, A., O'Neill, G., Wall, D., … Dwyer, R. M. (2013). miR-379 regulates cyclin B1 expression and is decreased in breast cancer. *PLoS One*, *8*(7), e68753.

Kreis, N. N., Sanhaji, M., Kramer, A., Sommer, K., Rodel, F., Strebhardt, K., & Yuan, J. (2010). Restoration of the tumor suppressor p53 by downregulating cyclin B1 in human papillomavirus 16/18-infected cancer cells. *Oncogene*, *29*(41), 5591–5603.

Lin, Q. J., Yang, F., Jin, C., & Fu, D. L. (2015). Current status and progress of pancreatic cancer in China. *World Journal of Gastroenterology*, *21*(26), 7988–8003.

Liu, J., Zhang, C., Hu, W., & Feng, Z. (2015). Tumor suppressor p53 and its mutants in cancer metabolism. *Cancer Letters*, *356*(2 Pt A), 197–203.

Liu, S. X., Xia, Z. S., & Zhong, Y. Q. (2014). Gene therapy in pancreatic cancer. *World Journal of Gastroenterology*, *20*(37), 13343–13368.

Lujambio, A., Akkari, L., Simon, J., Grace, D., Tschaharganeh, D. F., Bolden, J. E., … Lowe, S. W. (2013). Non-cell-autonomous tumor suppression by p53. *Cell*, *153*(2), 449–460.

Mendoza, M., Mandani, G., & Momand, J. (2014). The MDM2 gene family. *Biomolecular Concepts*, *5*(1), 9–19.

Mohammed, S., Van Buren, G., 2nd, & Fisher, W. E. (2014). Pancreatic cancer: Advances in treatment. *World Journal of Gastroenterology*, *20*(28), 9354–9360.

Morton, J. P., Timpson, P., Karim, S. A., Ridgway, R. A., Athineos, D., Doyle, B., … Sansom, O. J. (2010). Mutant p53 drives metastasis and overcomes growth arrest/senescence in pancreatic cancer. *Proceedings of the National Academy of Sciences of the United States of America*, *107*(1), 246–251.

Nimeus-Malmstrom, E., Koliadi, A., Ahlin, C., Holmqvist, M., Holmberg, L., Amini, R. M., … Fjallskog, M. L. (2010). Cyclin B1 is a prognostic proliferation marker with a high reproducibility in a population-based lymph node negative breast cancer cohort. *International Journal of Cancer*, *127*(4), 961–967.

Pagani, I. S., Spinelli, O., Mattarucchi, E., Pirrone, C., Pigni, D., Amelotti, E., … Porta, G. (2014). Genomic quantitative real-time PCR proves residual disease positivity in more than 30% samples with negative mRNA-based qRT-PCR in Chronic Myeloid Leukemia. *Oncoscience*, *1*(7), 510–521.

Rossi, M. L., Rehman, A. A., & Gondi, C. S. (2014). Therapeutic options for the management of pancreatic cancer. *World Journal of Gastroenterology*, *20*(32), 11142–11159.

Sandvik, O. M., Soreide, K., Gudlaugsson, E., Kvaloy, J. T., & Soreide, J. A. (2016). Epidemiology and classification of gastroenteropancreatic neuroendocrine neoplasms using current coding criteria. *The British Journal of Surgery*, *103*(3), 226–232.

Shin, J. U., Lee, C. H., Lee, K. T., Lee, J. K., Lee, K. H., Kim, K. M., … Rhee, J. C. (2012). Prognostic significance of ATM and cyclin B1 in pancreatic neuroendocrine tumor. *Tumour Biology*, *33*(5), 1645–1651.

Singh, R., Nawale, L., Sarkar, D., & Suresh, C. G. (2016). Two chitotriose-specific lectins show anti-angiogenesis, induces caspase-9-mediated apoptosis and early arrest of pancreatic tumor cell cycle. *PLoS One*, *11*(1), e0146110.

Sivonova, M. K., Vilckova, M., Kliment, J., Mahmood, S., Jurecekova, J., Dusenkova, S., … Dobrota, D. (2015). Association of p53 and p21 polymorphisms with prostate cancer. *Biomedical Reports*, *3*(5), 707–714.

Srivastava, S. K., Bhardwaj, A., Arora, S., Tyagi, N., Singh, S., Andrews, J., … Singh, A. P. (2015). MicroRNA-345 induces apoptosis in pancreatic cancer cells through potentiation of caspase-dependent and -independent pathways. *British Journal of Cancer*, *113*(4), 660–668.

Sun, Y., Yang, S., Sun, N., & Chen, J. (2014). Differential expression of STAT1 and p21 proteins predicts pancreatic cancer progression and prognosis. *Pancreas*, *43*(4), 619–623.

Suzuki, H., Ito, R., Ikeda, K., & Tamura, T. A. (2012). TATA-binding protein (TBP)-like protein is required for p53-dependent transcriptional activation of upstream promoter of p21Waf1/Cip1 gene. *The Journal of Biological Chemistry*, *287*(24), 19792–19803.

Wang, Z., Fan, M., Candas, D., Zhang, T. Q., Qin, L., Eldridge, A., … Li, J. J. (2014). Cyclin B1/Cdk1 coordinates mitochondrial respiration for cell-cycle G2/M progression. *Developmental Cell*, *29*(2), 217–232.

Wolfgang, C. L., Herman, J. M., Laheru, D. A., Klein, A. P., Erdek, M. A., Fishman, E. K., & Hruban, R. H. (2013). Recent progress in pancreatic cancer. *CA: A Cancer Journal for Clinicians*, *63*(5), 318–348.

Wong, V. C., Morse, J. L., & Zhitkovich, A. (2013). p53 activation by Ni(II) is a HIF-1alpha independent response causing caspases 9/3-mediated apoptosis in human lung cells. *Toxicology and Applied Pharmacology*, *269*(3), 233–239.

Yadav, D., & Lowenfels, A. B. (2013). The epidemiology of pancreatitis and pancreatic cancer. *Gastroenterology*, *144*(6), 1252–1261.

Zhang, H., Li, X., Meng, W., Zhang, L., Zhu, X., Bai, Z., … Zhou, W. (2018). Overexpression of p16ink4a regulates the Wnt/betacatenin signaling pathway in pancreatic cancer cells. *Molecular Medicine Reports*, *17*(2), 2614–2618.

Zhang, J. J., Zhu, Y., Yang, C., Liu, X., Peng, Y. P., Jiang, K. R., … Xu, Z. K. (2016). Yin Yang-1 increases apoptosis through Bax activation in pancreatic cancer cells. *Oncotarget*, *7*(19), 28498–28509.

Zhang, Y., Zhang, Y. J., Zhao, H. Y., Zhai, Q. L., Zhang, Y., & Shen, Y. F. (2014). The impact of R213 mutation on p53-mediated p21 activity. *Biochimie*, *99*, 215–218.

Zhao, H., Wang, Q., Wang, X., Zhu, H., Zhang, S., Wang, W., … Huang, J. (2016). Correlation between RAB27B and p53 expression and overall survival in pancreatic cancer. *Pancreas*, *45*(2), 204–210.

Zhou, L., Li, J., Zhao, Y. P., Cui, Q. C., Zhou, W. X., Guo, J. C., … Zhang, T. P. (2014). The prognostic value of Cyclin B1 in pancreatic cancer. *Medical Oncology*, *31*(9), 107.

How to cite this article: Zhang H, Zhang X, Li X, et al. Effect of CCNB1 silencing on cell cycle, senescence, and apoptosis through the p53 signaling pathway in pancreatic cancer. *J Cell Physiol*. 2018;1–13. https://doi.org/10.1002/jcp.26816